



Optics Letters

Self-assembled micropillars fabricated by holographic femtosecond multi-foci beams for *in situ* trapping of microparticles

YANLEI HU,¹  WENFEI FENG,¹ CHENG XUE,¹ ZHAOXIN LAO,^{1,2} SHENGYUN JI,¹ ZE CAI,¹ WULIN ZHU,¹ JIAWEN LI,¹  DONG WU,^{1,3} AND JIARU CHU¹

¹CAS Key Laboratory of Mechanical Behavior and Design of Materials, Key Laboratory of Precision Scientific Instrumentation of Anhui Higher Education Institutes, Department of Precision Machinery and Precision Instrumentation, University of Science and Technology of China, Hefei 230026, China

²e-mail: laoxx@ustc.edu.cn

³e-mail: dongwu@ustc.edu.cn

Received 27 May 2020; revised 6 July 2020; accepted 8 July 2020; posted 14 July 2020 (Doc. ID 398682); published 18 August 2020

Dynamic self-assembly of micropillars has found wide applications in targeted trapping, micro-crystallization and plasmonic sensing. Yet the efficient fabrication of micropillars array with high flexibility still remains a grand challenge. In this Letter, holographic femtosecond laser multi-foci beams (fs-MFBs) based on a spatial light modulator (SLM) is adopted to efficiently create micropillars array with controllable geometry and spatial distribution by predesigning the computer-generated holograms (CGHs). Based on these micropillars array, diverse hierarchical assemblies are formed under the evaporation-induced capillary force. Moreover, taking advantage of the excellent flexibility and controllability of fs-MFBs, on-demand one-bead-to-one-trap of targeted microspheres at arbitrary position is demonstrated with unprecedentedly high capture efficiency, unfolding their potential applications in the fields of microfluidics and biomedical engineering. © 2020

Optical Society of America

<https://doi.org/10.1364/OL.398682>

It is a pervasive phenomenon at the macroscale that filaments can self-assemble actuated by capillary force, such as hairs or paintbrushes pulling out from water. As scale reducing to micro/nanoscale, the capillary force is inclined to overwhelm the standing force withstanding the bend of materials, which leads to collapse or spontaneous assembly of micropillars [1]. Some measures have been taken, for example, supercritical-point drying [2], to avoid this undesired and intractable phenomenon in preparation of high-aspect-ratio microstructures. At the same time, there have been a few enlightening studies to uncover the mechanism of capillarity-induced self-assembly at the mesoscale or nanoscale and explore its applications in preparing hierarchical and multifunctional structures [3–5].

The past few decades have witnessed the combination of capillarity-induced self-assembly and other micro/nano fabrication methods, such as replica molding [6], electron-beam lithography [7], multibeam laser interference [8], deep dry

etching [9], and direct laser writing [10,11] in order to create functional architectures. Among these methods, direct laser writing has enormous advantages in fabricating complex 3D devices due to its simplicity, high flexibility, and strong controllability [12–15]. However, the low throughput and low efficiency of the single laser beam writing strategy restricts its practical batch applications, e.g. in real-time *in-situ* target trapping [16]. Compared with direct laser writing of 3D microstructures, the self-assembly method possesses the merit of simplicity because only simple straight pillars are constructed for assembly of complicated microstructures. Therefore, the simple laser fabrication facilitates the integration of the parallel writing method to further enhance the fabrication efficiency. In recent years, various parallel laser processing techniques based on a microlens array (MLA) [17,18] or diffractive optical elements (DOEs) [19,20] have been developed to enhance the fabrication efficiency. The drawbacks of these techniques lie in the low flexibility because the multi-foci pattern is fixed once the optical elements (MLAs or DOEs) are manufactured. It is desirable that the spatial arrangement of multiple foci can be freely controlled on demand without unwieldy changing of the optical apparatus. Phase modulation with a spatial light modulator (SLM) has been proved to be able to flexibly split the laser beam into multi-foci beams (MFBs) [21,22], which have been adopted in various fields, such as laser beam shaping [23], optical tweezer [24], and microscale medical devices fabrication [25]. By changing the holograms encoded on the SLM, the spatial position and number of multi-foci spots can be easily regulated without additional optical or mechanical devices. Besides, the light intensity of each beam spot can be independently adjusted. These advantages enable the holographic MFB a promising approach for micropillar array fabrication.

Here, we combine the femtosecond (fs)-MFBs technique with capillarity-induced self-assembly to efficiently prepare hierarchical microstructures. The geometric parameters and spatial distribution of the micropillars can be easily regulated by controlling the multi-foci spots. On this basis, a diverse library of self-assembled microarchitectures is obtained. Moreover, as

a proof of concept demonstration, an *in-situ* trapping strategy with ultrahigh efficiency for targeted capturing of microparticles at arbitrary position is achieved, showcasing the potential of this technology in microfluidic applications and biomedical engineering.

Figure 1(a) depicts the experimental setup for fabricating micropillars with MFBs. First, the weighted Gerchberg–Saxton (GSW) algorithm [26] is adopted to design the CGH of MFBs and then, a superposition with a blazed grating (BG) is performed on the CGH for shifting the desired multi-foci pattern away from the zero-order diffraction light. The phase profile of BG can be expressed by $2\pi x/\Delta$, where Δ represents the period of the BG. After collimation, a femtosecond laser (central wavelength, 800 nm; repetition rate, 80 MHz; pulse width, 75 fs) illuminates a reflective liquid-crystal SLM (Pluto NIR-II, Holoeye, 1920×1080 pixels, 256 gray levels, pixel pitch of $8 \mu\text{m}$) encoded with the CGH, then passes through a 4-f optical system and focused by a $50\times$ objective lens (NA: 0.8). The unwanted zero-order diffraction light is filtered out and the desired first-order diffraction beam is selectively introduced into the microscope system. The multi-foci spots can be observed in the focal plane of the objective. Figure 1(b) shows the simulated (upper) and experimental (lower) light field intensity distribution of 4-foci MFBs. The sample is inversely mounted on a 3D piezoelectric stage (P545, Physik Instrumente, traveling range: $200 \mu\text{m} \times 200 \mu\text{m} \times 200 \mu\text{m}$) and micropillars are processed in the photoresist (SZ2080, IESL-FORTH, Greece) by two-photon polymerization (TPP). The whole process is monitored by a CCD camera. The average laser power of each beam in fs-MFBs for polymerization is $\sim 14 \text{ mW}$. The height of micropillars is adjusted by moving the piezoelectric stage in vertical direction during TPP, while the distance between them is determined by the predesigned CGH. A micropillars array

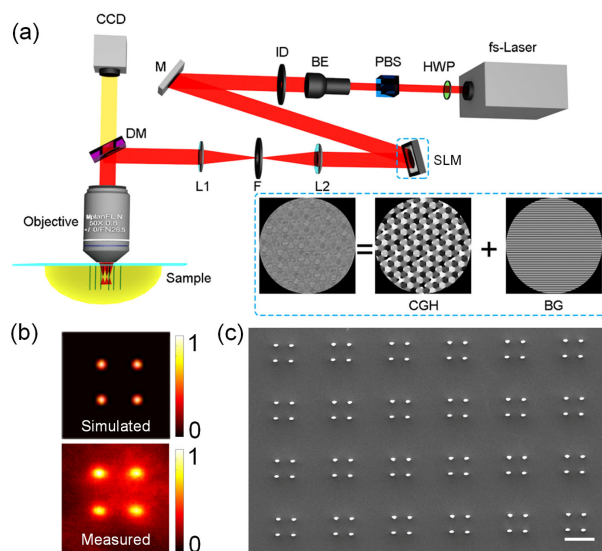


Fig. 1. Fabrication of micropillars with MFBs based on SLM. (a) Sketch of the experimental setup. The inset illustrates the design of CGH. HWP: half-wave plate; PBS: polarizing beam splitter; BE: beam expander; ID: iris diaphragm; M: mirror; SLM: spatial light modulator; L: lens; CCD: charge-coupled device; DM: dichroic mirror. (b) The simulated (top) and experimental (down) light field intensity distribution of a four-foci MFBs. (c) Top-view SEM image of micropillars array fabricated by the MFBs as shown in (b), scale bar: $10 \mu\text{m}$.

fabricated by 4-foci MFBs is shown in Fig. 1(c). Due to the high efficiency of the multi-foci parallel fabrication strategy, each four-pillar cell can be rapidly accomplished within 0.5 s.

The principle for self-assembly of micropillars is illustrated in Fig. 2(a). After fabrication, the sample is put into a developer (1-propanol) for about 30 min to wash away the unpolymerized photoresist and then taken out for the evaporation of liquid. A meniscus arises between two adjacent micropillars when the liquid surface reaches the top of the micropillars, leading to the capillary force $F_c \sim \gamma S \cos \theta/d$, where γ is the interfacial tension of the liquid, S is the effective solid-liquid contact area determined by the pillar radius r , θ is the contact angle, and d is the distance between two neighboring micropillars. The bending of the pillars triggers an elastic restoring force to resist the capillary force, $F_s \sim Er^4 d/h^3$, where E and h represents Young's modulus and the height of the micropillars, respectively [27], as depicted in Fig. 2(b). In our study, these three parameters: E , θ , and r are assumed to be constants because the same photoresist and developer are used for fabrication, and the power of each beam in the MFBs is controlled to be the same value. Our research focuses on the effect of the geometric parameters (height and distribution) of pillars on the yield ratio of capillarity-induced self-assembly. The formula of the elastic standing force shows that F_s is inversely proportional to the cube of height h . Hence, if the distance d is fixed, the short pillars can remain upright due to strong F_s in the drying process, whereas the high pillars bend to their neighbors because of a relatively weak F_s . In order to make the MFBs-assisted capillarity-induced self-assembly a controllable approach to construct hierarchical structures for further applications, it is necessary to regulate the relationship between F_c and F_s for realizing highly-ordered self-assembled structures. As shown in Fig. 2(d), it is revealed that both the height h and distance d play important roles in the yield ratio of the self-assemblies. When d is $4 \mu\text{m}$ and h ranges from 2 to $8 \mu\text{m}$, the yield rate remains above 90%, revealing high reliability of the MFBs-assisted capillarity-induced self-assembly method with appropriate parameters. When d is $5 \mu\text{m}$, only $\sim 20\%$ of pillars assemble into four-pillar cells with $h = 2 \mu\text{m}$, and the yield rate of four-pillars cells rises to 90% as h increases to $8 \mu\text{m}$. The trend is similar to that with d of $6 \mu\text{m}$. High yield ratio ($>90\%$) can be obtained when $d = 6 \mu\text{m}$ and $h > 6 \mu\text{m}$.

Combining the designability of MFBs with the high flexibility of the femtosecond laser printing technique, the spatial distribution of micropillars can be easily regulated for constructing diverse complex hierarchical assemblies based on the spontaneous capillary force. Figure 3 shows a series of assemblies with multi-element cells. The four pillars in the two adjacent two-pillar cells as shown in Fig. 3(a) are processed by four-foci MFBs with an exposure, the top-right inset is the simulated optical field for four-foci MFBs at the focal plane. By changing the MFBs via regulating CGHs, self-assemblies with different numbers of micropillars and various spatial distributions can be created. Each unit in Figs. 3(a)–3(e) can be called a single-level assembly for the reason that all the pillars in a unit have the same height. Figure 3(f) presents an example of two-level assembly. From the oblique SEM image, we can clearly see that a two-level assembly contains pillars with different heights. In this case, five-foci MFBs are utilized to fabricate the five pillars with the height of $8 \mu\text{m}$, and 12-foci MFBs are used to fabricate the 12 pillars with the height of $3 \mu\text{m}$. During evaporation, the surface

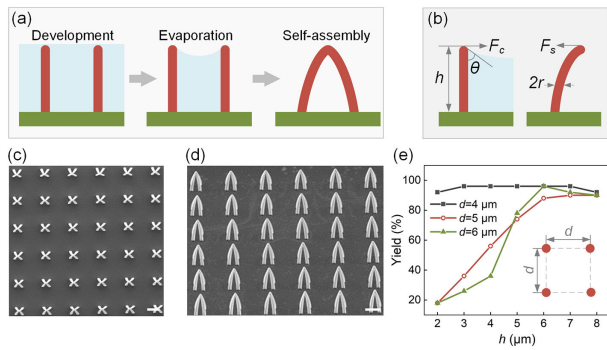


Fig. 2. Capillary force driven controllable self-assembly of MFBs-processed micropillars. (a) Process of the micropillars self-assembly. (b) Schematic of the capillary force F_c and standing force F_s acting on the micropillars during the evaporation. (c) Top-view SEM image of the four-pillar assemblies. (d) Oblique view SEM image of the microassemblies, scale bars: 10 μm . (e) The line chart reveals the influence of height h and distance d on the yield rate of the four-pillar assembly. The inset shows the spatial distribution of the four pillars.

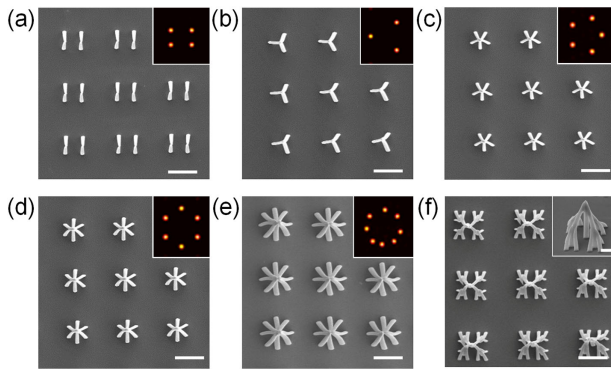


Fig. 3. Diverse ordered micro-assemblies constructed by the MFBs. (a)–(e) SEM images of two-pillar, three-pillar, five-pillar, six-pillar, and eight-pillar cells, respectively. The insets show the simulated light field of predesigned MFBs for pillar cell fabrication. (f) Two-level hierarchical microstructures consisting of 17 pillars. Five pillars with height of 8 μm are formed by five-foci MFBs while the other twelve pillars with height of 3 μm are formed by 12-foci MFBs. Scale bars: 10 μm . Inset: oblique view SEM image of a single assembled structure, scale bar: 2 μm .

of the liquid gradually decreases, so that the five higher pillars firstly collapse together and subsequently the 12 shorter pillars bend to the neighboring higher pillars, resulting in a branch-shape two-level assembly. Based on this principle, much more complex hierarchical assemblies can be generated using the MFBs-assisted capillarity-induced self-assembly.

The trapping of objects of interest is crucial in a wide range of research fields such as single-cell analysis in biomedical engineering [28], and the localized nucleating and crystallization in chemistry [29], to name a few. Despite the fact that optical tweezers are successfully explored for manipulating tiny objects and cells with different sizes ranging from tens of nanometers to micrometers, a mechanical trapping strategy is needed for the cases where laser beam may cause potential damage to living specimen or interference to chemical reactions. For example, the robotic grippers triggered by temperature [30],

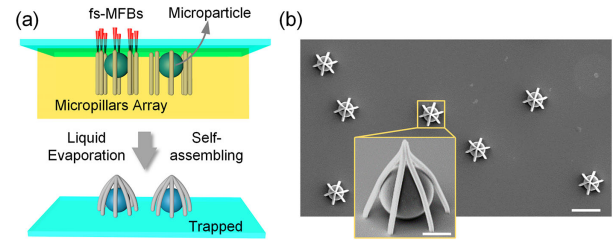


Fig. 4. Application of the MFBs-enabled micro-assemblies in trapping microparticles. (a) Schematic illustration of the *in-situ* trapping process. (b) SEM image shows the efficient and *in-situ* trapping of 10 μm SiO_2 microparticles by the six-pillar structures. Scale bar: 20 μm . Each SiO_2 particle is finely captured by one assembled structure as shown in inset. Scale bar: 5 μm .

magnetic force [31], and chemicals [32] have been investigated to fulfill these requirements. The previous studies have demonstrated the application of self-assembled micropillars in trapping microparticles [8,9]. However, the capture efficiency is limited in these methods. In other words, only a portion of grippers can successfully trap the target microparticles while others remain unoccupied. Besides, in these methods the self-assembled micropillars are prepared before trapping operations, thus they are not *in-situ* tunable according to the locations and dimensions of the targets, resulting in loss of some important information. In real implementations, most of the micro-targets distribute arbitrarily across the specimen. Herein we demonstrate that the assembled micropillars fabricated by fs-MFBs are capable of capturing microparticles with high efficiency as well as the targeted “one-bead-to-one-trap” ability.

The concept of *in-situ* targeted trapping is depicted in Fig. 4(a). 10 μm SiO_2 microparticles are dispersed in the liquid-phase photosensitive resist for demonstration of *in-situ* target trapping at arbitrary position. The prepared sample is inversely fixed on a piezoelectric stage. Guided by real-time image monitoring, 6-foci MFBs are applied to fabricate 15 μm -high pillars to rapidly encircle the individual targeted SiO_2 particles one by one in the sample. After the subsequent development process, the cage-like assembling units composed of six bent pillars by capillarity-induced self-assembly finally trap the selected microparticles of interest, as shown in Fig. 4(b). Each micro-cage traps a single microparticle by using this method. It is worth noting that ultrahigh capture efficiency is easily realized using this strategy, and microparticles at arbitrary position can be trapped rapidly.

In conclusion, spatial light modulation technique is utilized to generate fs-MFBs for efficient fabrication of micropillars which subsequently self-assemble into hierarchical structures driven by capillary force. Owing to the high flexibility of the fs-MFBs technique, micropillars with specific spatial distributions can be fabricated by switching the predesigned CGHs, so that diverse ordered hierarchical structures can be obtained. Furthermore, the efficient *in situ* trapping of microparticles at arbitrary positions is realized by using the assembled micropillars by fs-MFBs, opening up a wide range of possibilities in the fields of microfluidics, biomedicine, and chemistry.

Funding. National Natural Science Foundation of China (51675503, 51805509, 51875544, 61805230, 91963127); USTC Research Funds of the Double First-Class

Initiative (YD2090002005); Youth Innovation Promotion Association of the Chinese Academy of Sciences (2017495); National Key Research and Development Program of China (2018YFB1105400).

Acknowledgment. We acknowledge the Experimental Center of Engineering and Material Sciences at USTC for the fabrication and measuring of samples. This work was partly carried out at the USTC Center for Micro and Nanoscale Research and Fabrication.

Disclosures. The authors declare no conflicts of interest.

REFERENCES

1. A. J. Storm, J. H. Chen, X. S. Ling, H. W. Zandbergen, and C. Dekker, *Nat. Mater.* **2**, 537 (2003).
2. J. M. DeSimone, *Science* **297**, 799 (2002).
3. M. De Volder, S. H. Tawfick, S. J. Park, D. Copic, Z. Zhao, W. Lu, and A. J. Hart, *Adv. Mater.* **22**, 4384 (2010).
4. D. Wu, Q. D. Chen, B. B. Xu, J. Jiao, Y. Xu, H. Xia, and H. B. Sun, *Appl. Phys. Lett.* **95**, 091902 (2009).
5. J. Ni, Z. Wang, Z. Li, Z. Lao, Y. Hu, S. Ji, B. Xu, C. Zhang, J. Li, D. Wu, and J. Chu, *Adv. Funct. Mater.* **27**, 1701939 (2017).
6. D. Chandra, J. A. Taylor, and S. Yang, *Soft Matter* **4**, 979 (2008).
7. H. Duan and K. K. Berggren, *Nano Lett.* **10**, 3710 (2010).
8. D. Wu, S.-Z. Wu, S. Zhao, J. Yao, J.-N. Wang, Q.-D. Chen, and H.-B. Sun, *Small* **9**, 760 (2013).
9. B. Pokroy, S. H. Kang, L. Mahadevan, and J. Aizenberg, *Science* **323**, 237 (2009).
10. Y. Hu, Z. Lao, B. P. Cumming, D. Wu, J. Li, H. Liang, J. Chu, W. Huang, and M. Gu, *Proc. Natl. Acad. Sci. USA* **112**, 6876 (2015).
11. Z. Lao, Y. Hu, C. Zhang, L. Yang, J. Li, J. Chu, and D. Wu, *ACS Nano* **9**, 12060 (2015).
12. M. Malinauskas, A. Žukauskas, S. Hasegawa, Y. Hayasaki, V. Mizeikis, R. Buividas, and S. Juodkazis, *Light Sci. Appl.* **5**, e16133 (2016).
13. K. Sugioka and Y. Cheng, *Light Sci. Appl.* **3**, e149 (2014).
14. Y. Hu, Z. Wang, D. Jin, C. Zhang, R. Sun, Z. Li, K. Hu, J. Ni, Z. Cai, D. Pan, X. Wang, W. Zhu, J. Li, D. Wu, L. Zhang, and J. Chu, *Adv. Funct. Mater.* **30**, 1907377 (2020).
15. J. Yang, F. Luo, T. S. Kao, X. Li, G. W. Ho, J. Teng, X. Luo, and M. Hong, *Light Sci. Appl.* **3**, e185 (2014).
16. B. Xu, Y. Shi, Z. Lao, J. Ni, G. Li, Y. Hu, J. Li, J. Chu, D. Wu, and K. Sugioka, *Lab Chip* **18**, 442 (2018).
17. J.-I. Kato, N. Takeyasu, Y. Adachi, H.-B. Sun, and S. Kawata, *Appl. Phys. Lett.* **86**, 044102 (2005).
18. Y. Li and M. Hong, *Laser Photon. Rev.* **14**, 1900062 (2020).
19. X.-Z. Dong, Z.-S. Zhao, and X.-M. Duan, *Appl. Phys. Lett.* **91**, 124103 (2007).
20. F. Atry, E. Rentschler, S. Alkmin, B. Dai, B. Li, K. W. Eliceiri, and P. J. Campagnola, *Opt. Express* **28**, 2744 (2020).
21. H. Takahashi, S. Hasegawa, A. Takita, and Y. Hayasaki, *Opt. Express* **16**, 16592 (2008).
22. K. Obata, J. Koch, U. Hinze, and B. N. Chichkov, *Opt. Express* **18**, 17193 (2010).
23. E. Frumker and Y. Silberberg, *Opt. Lett.* **32**, 1384 (2007).
24. J. E. Curtis, B. A. Koss, and D. G. Grier, *Opt. Commun.* **207**, 169 (2002).
25. S. D. Gittard, A. Nguyen, K. Obata, A. Koroleva, R. J. Narayan, and B. N. Chichkov, *Biomedical Opt. Express* **2**, 3167 (2011).
26. R. Di Leonardo, F. Ianni, and G. Ruocco, *Opt. Express* **15**, 1913 (2007).
27. D. Chandra and S. Yang, *Langmuir* **25**, 10430 (2009).
28. D. Martella, S. Nocentini, D. Nuzhdin, C. Parmeggiani, and D. S. Wiersma, *Adv. Mater.* **29**, 1704047 (2017).
29. Y. Hu, Y. Zhang, H. Yuan, R. Wang, S. Jiang, Z. Lao, G. Li, D. Wu, J. Li, and J. Chu, *Appl. Phys. Lett.* **113**, 251904 (2018).
30. A. Azam, K. E. Laffin, M. Jamal, R. Fernandes, and D. H. Gracias, *Biomed. Microdevices* **13**, 51 (2011).
31. M. S. Sakar, E. B. Steager, D. H. Kim, M. J. Kim, G. J. Pappas, and V. Kumar, *Appl. Phys. Lett.* **96**, 043705 (2010).
32. N. Bassik, A. Brafman, A. M. Zarafshar, M. Jamal, D. Luvsanjav, F. M. Selaru, D. H. Gracias, and J. Am, *J. Am. Chem. Soc.* **132**, 16314 (2010).